SEVENTH EUROPEAN ROTORCRAFT AND POWERED LIFT AIRCRAFT FORUM

Paper No. 77

# OPTIMIZATION OF BLADE PITCH ANGLE FOR HIGHER HARMONIC ROTOR CONTROL

H. G. Jacob

Institut für Flugführung der
Technischen Universität Braunschweig
Germany

G. Lehmann

Deutsche Forschungs- und Versuchsanstalt für Luft- und
Raumfahrt e.V., Institut für Flugmechanik
Braunschweig, Germany

September 8-11, 1981

Garmisch-Partenkirchen
Federal Republic of Germany

Deutsche Gesellschaft für Luft- und Raumfahrt e.V.
Goethestr. 10, D-5000 Köln 51, F.R.G.

# OPTIMIZATION OF BLADE PITCH ANGLE FOR HIGHER HARMONIC ROTOR CONTROL

H. G. Jacob

Institut für Flugführung der
Technischen Universität Braunschweig
Germany

G. Lehmann

Deutsche Forschungs- und Versuchsanstalt für Luft- und
Raumfahrt e.V., Institut für Flugmechanik
Braunschweig, Germany

## Abstract

This contribution describes a method which allows to optimize the higher harmonic blade pitch dependent on a quality criterion. Various specific design objectives can be included in this criterion.

The principle, the (computer supported) dynamic optimization procedure is based on the representation of the time dependent and distributed evolution of the control inputs by a system of mathematical functions. The coefficients of these functions are iterated by a static search algorithm to values which optimize the quality criterion associated with the task.

Three different mathematical models are used to show the effectiveness of higher harmonic blade control and to give an overview on the sensitivity of these control inputs.

## Notation

| | |
|---|---|
| $F_{nt}$ / $F_{wt}$ | without / with consideration of the trim state — value of the quality criterion |
| $I_b$ | flapping moment of inertia |
| $M^b$ | blade first moment of inertia |
| $M^g$ | moment of the spring |
| $M^s$ | moment of air loads |
| $V^\beta$ | helicopter velocity |
| $v_{io}$ | mean value of the induced velocity |
| $q$ | generalized coordinate |
| $\underline{\underline{\nu}}^2$ | diag. matrix formed by the scaled eigenvalues |
| $\mu$ | rotor advance ratio |
| $\lambda$ | rotor inflow ratio |
| $\theta$ | blade pitch angle |
| $\theta_o$ | collectiv pitch |
| $\theta_{tw}$ | linear twist rate |
| $\theta_c$ | pitch angle of the conventional control |
| $\theta^{add}$ | additional control inputs |
| $\Delta\psi^n$ | input amplitude of the n-th harmonic |
| $c_{i,j}$ | input phase of the n-th harmonic |
| | parameters in equation (4.1) |

## 1. Introduction

The application of higher harmonic control to helicopter rotors makes it possible to induce different effects, e.g.

- to reduce the oscillatory hub forces and moments
- to decrease the blade stresses
- to increase the performance
- to avoid instabilities of blade motion.

Dependent on the task it will be necessary to have a special kind of higher harmonic control. For a simulation it is also necessary to know the effect of control parameter variation. As it is almost impossible to investigate these relationships analytically it is a common practice to use numerical techniques e.g. ROMULAN [1], [2]. The only restriction of this computer program is, that linear relationships between the inputs and outputs are assumed. If influences of nonlinearities are not neglectible other methods must be applied. Therefore we use an optimization method to determine the optimal time dependent and in one task also locally distributed blade pitch angle. There are no restrictions for the mathematical model are necessary. The application of this optimization method is easy because the software interface is very simple.

Three different mathematical models are used to show the effectiveness of higher harmonic blade control and to give an overview on the sensitivity of these control inputs. The first computations are based on a mathematical model which describes a hingeless rotorsystem with rigid blades, an effective hinge offset and a hub restraint [3]. In the second step full elastic blades are used in conjunction with a mode shape method. The control inputs to these two models are only higher harmonic pitch angles for full-blade feathering. In the last model additional variable twist is used as the basis for minimizing the vibratory hub loads.

## 2. The Optimization Method [4], [6]

The computer supported optimization method which was applied to determine the optimal time dependent and, if desired, also locally distributed open-loop control of the blade pitch angle is neither elegant nor rigorous, but it is easy to use. The originally complicated dynamic optimization problem is transformed to a static parameter optimization task by expressing the time dependent and distributed evolution of the control inputs $u(t, z)$ by a given structure of mathematical functions. The unknown coefficients $c_i$ of these functions are then iterated by a static search algorithm [5] to values which optimize the quality criterion F associated with the behaviour of the rotor blade (Figure 1).

The following program parts are used for implementing the optimization procedure:

- The bloc with the structure of the time dependent and, if desired, locally distributed control inputs $u\ (t,z,c_i)$ delivers the commands for the system to be optimized, this in function of the coefficients $c_i$ given by the static optimization algorithm. For the computation of optimal blade pitch angles with regard to the minimization of the hub vibrations a structure was chosen comprising several higher harmonic terms in function of time and in addition a so called Tschebyscheff-polynomial in function of the distance along the axis of the rotor blade. The coefficients $c_i$ represent the amplitudes and the phase-shifts of the higher harmonic inputs and the factors for the Tschebyscheff-polynomial. This time dependent and locally distributed structure is added to the conventional sinusoidal control of the rotor blade's pitch angle.

- The program part with the mathematical model allows the simulation of the considered system under the influence of the input commands manipulated by the search algorithm. During the investigations about the effects of higher harmonic control two different models were used to describe the dynamical behaviour of the rotor system. The simpler model presumed a hingeless rotor arrangement with rigid blades. In the second model full elastic blades were implemented in conjunction with a mode shape method.

- The bloc named quality criterion computes a scalar value F representing the performance of the system to be optimized for a given set of input coefficients $c_i$. The quality criterion may comprise several different performance indexes added together with appropriate weighting parameters. In the case dealt here the design objective consists in minimizing the oscillations in the hub reactions - with respect to forces as well as moments - and to hold the mean values of these components in view to a desired steady state flight.

- The program part 'static optimization algorithm' has to drive iteratively the coefficients $c_i$ of the input structure to values minimizing the quality criterion. For the described studies a very simple optimization program [5] has been used, which comprises less than 100 FORTRAN-statements. Basically the algorithm stores at each iteration the evaluation F of the quality criterion and compares it with values previously determined. This comparision triggers a new selection of the coefficients $c_i$ in a particular way. The process is repeated until the performance index F ceases to change. Constraints may be taken into account either by adding penality functions to the quality criterion or by introducing boundaries directly into the search space over which the nonlinear programming algorithm operates.

- The main advantage of the described optimization strategy consists in its simple and flexible application. The method can be easily used because the originally dynamic optimization problem is solved by a given static search algorithm which needs not to be adapted to the task considered. The method is very flexible because the different program parts are independent from each other. This means that the mathematical model or the quality criterion or the structure of the input commands may be changed without the obligation to modify accordingly the other program parts, as it is often the case when using more difficult optimization methods.

## 3. Time Dependent Optimal Control of the Blade Pitch Angle

### 3.1 Mathematical Model of the Rotor with Rigid Blades and Flap Hinges

The numerical calculations with HHC are based on the design parameters from the model test rotor used in the Institut für Flugmechanik in the DFVLR Braunschweig.

| | |
|---|---|
| type | four-bladed, soft in-plane hingeless rotor |
| radius | 2. m |
| chord | 0.121 m |
| twist | -4 deg/m |
| air-foil | NACA 23012 |
| tip-speed | 218 m/s |

The blade mass distribution and stiffness distributions are shown in Figure 2.

For the first calculations a mathematical model with rigid blades and flapping hinges with torsional spring is used. So the flap motion is the only degree of freedom. The amount of hinge-offset and the torsional-spring strength were chosen to match the rotating and non-rotating natural frequencies of the true blade. For this model of hingeless blades the following nonlinear equation of motion is given

$$(3.1)\quad I_b\cdot\ddot{\beta}+\Omega^2\sin\beta\left(\cos\beta\cdot I_b+\frac{M_g}{g}\cdot eR\right)+M_g\cdot\cos\beta+M_s=M_\beta$$

with

$$I_b=R^3\int_e^1 m'(x-e)^2\,dx$$

$$M_g=g\cdot R^2\int_e^1 m'(x-e)\,dx$$

$$M_s=K_\beta\cdot\beta$$

$$M_\beta=R\int_e^1(x-e)\,dF_z$$

The aerodynamic loads of the rotor blades are calculated with the blade-element theory. For the estimation of the mean induced velocity we have used the Glauert formula

(3.2) $v_i = v_{io}(1+K_x \cdot x \cdot \cos\psi)$

where $v_{io}$ is the induced velocity at the rotor centre, taken as the result from the equation

$$v_{io} = \frac{T}{2\rho F(V^2+v_{io}^2)^{1/2}} .$$

In equ. (3.2) $K_x$ is the factor to calculate the longitudinal induced-velocity distribution and is given by

$$K_x = \frac{4/3\ \mu/\lambda}{1.2+\mu/\lambda} .$$

As we have used a rigid blade the local blade pitch angle can be written as

(3.3) $\theta = \theta_o + \theta_{tw} \cdot x + \theta_{lc} \cdot \cos\psi + \theta_{ls} \cdot \sin\psi$ .

This is a formula to calculate the conventional rotor blade control. For Higher Harmonic Control (HHC) equation (3.3) can be extended to

$$\theta = \theta_C + \sum_{n=2}^{\infty} (\theta_{nc} \cos n\psi + \theta_{ns} \sin n\psi)$$

or equivalent

(3.4) $$\theta = \theta_C + \sum_{n=2}^{\infty} \theta_n \cos(n\psi + \Delta\psi_n)$$

where $\theta_C$ is the blade pitch angle of the conventional rotor blade control (see equation (3.3)). Equation (3.4) is a formula for a general cyclic blade pitch variation, however, only the first higher harmonics including the fifth order are applied in this case.

Now the local incidence angle $\alpha$ of the blade can be written as

$$\alpha = \theta + \phi$$

where $\phi$ is the section inflow angle. To calculate the section lift and drag coefficients $c_l$ and $c_d$, we have used experimental results from the NACA 0012, shown in Figure 3 - 6. These data have been modified for the NACA 23012.

## 3.2 Results with the Rigid Blade Model and Single Higher Harmonic Blade Control

### 3.2.1 Results without Consideration of the Trim State

The structure of the quality criterion is mainly dependent upon the task. To minimize the oscillations of the hub forces and moments the following quality criterion is appropriate and was applied in the first calculations.

$$(3.5)\quad F_{nt} = \sum_{i=1}^{3} |F_{i,max} - F_{i,min}| + \sum_{i=1}^{3} |M_{i,max} - M_{i,min}| \ .$$

The scalar value F represents the sum of the oscillation amplitudes, $F_i$ the nonrotating hub forces X, Y, Z and $M_i$ the nonrotating hub moments L, M, N.

The optimization procedure starts at steady state flight conditions with an advance ratio $\mu$=0.318. For this state the control parameters in Table 1 are necessary. The corresponding oscillation amplitudes of the hub reactions are shown in Table 2.

In the calculations always one higher harmonic blade pitch variation was added to the conventional blade pitch control. The optimization algorithm drives the two parameters $\theta_n$ and $\Delta\psi_n$ to values which minimize the quality criterion $F_{nt}$. Results of these calculations are shown in Figure 7. The two beams on the left side represent the value $F_{nt}$ obtained by the conventional control. This value has been splitted into the components of the hub forces and moments.

Thus the different effects of the higher harmonic control inputs can better be demonstrated. It can be stated that oscillating hub forces are mainly reduced by the 3Ω, 4Ω and 5Ω blade pitch variation. The corresponding hub moments do not decrease in the same manner. The best reduction is obtainable with a 2Ω control, but a attendant phenomenon is the change of the trim conditions. Table 3 shows the mean values of the nonrotating hub forces and moments. The trim state is given in the first column and the values obtained by the optimal 2Ω blade pitch variation are presented in the second column.

It becomes obvious that there is a significant change in the pitch and roll moments together with a small increase in thrust. This effect can be explained with a wide-band reaction in the aerodynamic loads due to a single frequency oscillation of the angle of incidence. Figure 8 shows the results of a linearized approximation of the lift caused by a 4Ω blade pitch variation. If we vary the pitch angle with 2Ω the influence to the 1Ω airloads is not negligible, but it decreases with the higher orders. This is confirmed by numerical results. When 3Ω, 4Ω and 5Ω control is used there are only small changes in the trim conditions.

To summarize the results we always have a decrease in the oscillatory hub forces and moments. The improvement of the value $F_{nt}$ is about 33% with the 3Ω control, 38.5% with the 4Ω control, and 15% with the 5Ω control. Figure 7 presents the required control inputs. It can be seen that there is a unique decrease of the pitch angle.

### 3.2.2 Results with Consideration of the Trim State

The quality criterion in the foregoing calculations does not consider the trim conditions. The following criterion is defined to suppress the deviations in the steady hub forces and moments.

$$F_{wt} = \Big[\sum_{i=1}^{3} (F_{i,max}-F_{i,min})^2+(M_{i,max}-M_{i,min})^2 + \sum_{i=1}^{3} 5\cdot(F_{i,mc}-F_{i,ma})^2+5\cdot(F_{i,mc}-M_{i,ma})^2\Big]^{1/2} \tag{3.6}$$

with

$F_{i,max}$ = maximal value of the i-th hub force
$F_{i,min}$ = corresponding minimal value
$M_{i,max}$ = maximal value of the i-th hub moment
$M_{i,min}$ = corresponding minimal value
$F_{i,mc}$ = mean reference value of the i-th hub force
$M_{i,mc}$ = mean reference value of the i-th hub moment
$F_{i,ma}$ = actual mean value of the i-th hub force
$M_{i,ma}$ = actual mean value of the i-th hub moment.

This structure of the quality criterion allows the minimization of the oscillating hub forces and moments under the constraint that a desired steady state is warranted.

The additional control inputs can be described with the following formula:

$$\theta = \theta_C+\theta_{o,add.}+\sum_{n=1}^{5}\theta_n \cos(n\psi+\Delta\psi_n) = \theta_C+\theta_{add.} \tag{3.7}$$

with (n>=2)= number of the single higher harmonic applied to the rotor blade.

In this formula also a constant value $\theta_{o,add.}$ and the amplitude $\theta_1$ and phase shift $\Delta\psi_1$ of the first, the basic harmonic oscillation, are used for the optimization in view to hold the desired permanent status of operation (see the structure of the qualtity criterion).

In Figure 9 the percentual reductions of the hub reaction fluctuations in forces and moments are shown for the different single higher harmonic controls. The shaded beams symbolize the sum of the force fluctuations, the white beams the sum of the fluctuations in moments.

a.) Results with 2nd HHC

The optimization runs based on the mathematical model with the rigid rotor blade described in the paragraph 3.1 and minimizing the quality criterion defined in the paragraph 3.3.2 yielded the following results for a 2nd higher harmonic control:

$$\theta_{add.} = -0.006^{\circ} - 0.017^{\circ}\cos(\psi - 6.27^{\circ}) - 0.100^{\circ}\cos(2\psi + 23.56^{\circ}) \ .$$

As explained in the foregoing paragraph the constant value and the values associated with the basic harmonic control of the above equation are adapted by the optimization algorithm in a way to obtain the desired steady state flight which would be disturbed if only the 2nd HHC had been applied. The amplitude of the 2nd HHC has been driven by the search algorithm to a very low value of $\theta_2 = -0.100^{\circ}$ which yields only a small decrease of the quality criterion from $F_{wt}$=86.62 (conventional control) to $F_{wt}$=82.27 (2nd HHC). The sum of the fluctuations of the 6 hub reactions reduces from $F_{nt}$=196.78 to $F_{nt}$=181.45 as shown on Figure 9.

b.) Results with 3rd HHC

This structure of a supplementary control gives a very much better result with the following formula:

$$\theta_{add.} = 0.0 - 0.015^{\circ}\cos(\psi - 2.29^{\circ}) - 0.293^{\circ}\cos(3\psi + 3.77^{\circ}) \ .$$

The higher amplitude of $\theta_3 = -0.293^{\circ}$ of the 3rd HHC improves the quality criterion to $F_{wt}$=56.36 and lowers the sum of the fluctuations of the rotor components to $F_{nt}$=131.32 (see Table 4 in comparison with Table 2.).

The low values of the right column, namely the deviations of the actual mean values of the rotor components from the reference mean values, indicate that the desired flight condition is not altered by the additionally applied control on the rotor's blade pitch angle.

c.) Results with 4th HHC

When applying besides the correction for the basic harmonic control a supplementary 4th HHC with the following structure

$$\theta_{add.} = -0.001^{\circ} + 0.002^{\circ}\cos(\psi - 7.70^{\circ}) - 0.125^{\circ}\cos(4\psi - 22.17^{\circ})$$

then the amplitude $\theta_4 = -0.125^{\circ}$ of this 4th HHC delivers values of $F_{wt}$=58.25 and $F_{nt}$=135.97, which are similar to the results with 3rd HHC (see Figure 9).

d.) Results with 5th HHC

This optimization run yielded the additional input command

$$\theta_{add.} = -0.001^{o}+0.0003^{o}\cos(\psi+13.41^{o})+0.229^{o}\cos(5\psi+55.98^{o})$$

with the quality criterion $F_{wt}$=70.97 and the fluctuations sum of the hub components $F_{nt}$=168.11 which are worse values compared to the foregoing results.

## 3.3 Results with the Rigid Blade Model and Simultaneous Application of Several Higher Harmonics for the Blade Control

In this paragraph it will be shown what are the improvements in the reduction of vibrations when not single but several optimal higher harmonic controls are applied in function of time on the rotor blades.

### 3.3.1 Structure of the Additionally Applied Control

As described in paragraph 3.1 the control applied on the rotor blades comprises two parts. The first part consists in the unaltered conventional control, the second part delivers the additional control computed in a manner to diminish the fluctuations of the rotor forces and moments and to hold the desired flight path of the helicopter.

In the case dealt here the following structure of the additional control in function of time is used:

$$\theta_{add.} = \theta_{o} + \sum_{n=1}^{n_{max}} \theta_{n} \cos(n\psi+\Delta\psi_{n}) \tag{3.8}$$

with $n_{max}$=total number of harmonics simultaneously applied to the rotor blade.

As already mentioned the constant value $\theta_o$ and the coefficients $\theta_1$ and $\Delta\psi_1$ associated with the first basic harmonic are computed in a way to compensate the effects of the higher harmonics on the steady state flight characteristics of the helicopter.

### 3.3.2 Results with the simultaneous Application of Several HHCs

The Figure 10 demonstrates the percentual improvements in vibration suppressions when applying several HHCs simultaneously on the rotor blade. Again on the left side the beams symbolize the sum of the three fluctuations of the hub forces and on the right side the sum of the corresponding moments. It is visible that the second HHC besides the basic control yields only a small progress. The reduction in hub reaction oscillations is essential when using a blade control up to the 4th HHC. The sum of the hub reaction

fluctuations amounts only to a value of $F_{nt}$=103.7 compared with $F_{nt}$=136.0 when applying the 4th HHC alone. A supplementary 5th HHC does not improve the performance note-worthly (the most right beam will be explained in a further paragraph).

Figure 11 represents the oscillations of the hub reactions with more details. In each case (e.g. conventional control at the most left side) the force hub components fluctuations in x, y, and z direction are shown by the left side arrows and the corresponding moment fluctuations at the right side of each arrow group (dimensions N and N·m respectively).

On Table 5 the corresponding optimal higher harmonic controls are displayed in amplitude and phase shift. It is visible that in every case the amplitude for the 3rd HHC is the highest one.

Figure 12 shows the time evolution of the addionally applied pitch angle $\theta_{add.}(\psi)$ over one revolution of a rotor blade when a control up to the 4th HHC is applied. The resulting new total control $\theta$, this is the sum of the conventional and the additional command, is likewise represented (observe the different scales).

On this Figure it is clearly visible that the 3rd HHC gives the highest amplitude for the evolution of $\theta_{add.}(\psi)$, as expected by the values of Table 5.

The results in the reduction of the hub reaction oscillations are demonstrated on Table 6 . The quality criterion is improved to a value of $F_{wt}$=44.17 and the sum of the rotor component fluctuations is diminished to $F_{nt}$=103.69, as already mentioned.

### 3.4 Mathematical Model of the Rotor System with Full Elastic Blades

For further calculations the true rotor system was described by a mathematical model with full elastic blades to show the influence to the optimal control parameters. The full coupled mode shapes and the eigenvalues have been calculated with a finite element program [ 7 ], see Figure 13 . The forced blade motion then was computed with a mode shape method considerating the first flap mode and the first lag mode. So the equation of motion becomes

$$\ddot{\underline{q}} + \underline{\nu}^2 \underline{q} = \frac{1}{I} \underline{\Phi}^T \underline{F}(q,\dot{q},t)$$

The term $F(q,\dot{q},t)$ includes the aerodynamic forces and the coriolis forces, $\underline{\Phi}^T$ is the transposed modal matrix and I the generalized mass, normalized to the value 1. The aerodynamic forces have been calculated in the same manner shown in paragraph 3.1. The formula to determine the blade

pitch angle must be extended to

$$\theta=\theta_o+\theta_{tw}\cdot x+\theta_{1s}\sin\psi+\theta_{1c}\cos\psi+\theta_e+\theta_{HHC}$$

where $\theta_e$ is the blade pitch angle induced by the elastic deformation. Caused by the elastic deformations different conventional control inputs are required for this model to obtain the same trim conditions as in chapter 3.1. These new values are given in Table 1.

### 3.5 Results with a Full Elastic Blade Model and Single Higher Harmonic Blade Control

The optimization runs minimizing the quality criterion defined in chapter 3.1 yielded results shown in Figure 14 . Analogous to the model with rigid blades a 2Ω blade feathering decrease the quality criterion to the smallest value, but simultaneously distinct deviations in the trim conditions are obtained. The control inputs with lower frequencies (2Ω and 3Ω) have a mainly influence the oscillating hub moments in comparison to the 3Ω, 4Ω and 5Ω blade feathering minimizing the oscillating hub forces. In Figures 15-16 the results from the rigid blade and elastic blade model are displayed. The improvement of the quality criterion was about 39% for the 3Ω, 30% for the 4Ω and about 28% for the 5Ω blade feathering.

The results of both mathematical models have the same tendency, however with deviations in the quantities.

## 4. Time Dependent and Locally Distributed Optimal Control of the Blade Pitch Angle

After describing the improvements in the reduction of the hub reaction oscillations with single and with several simultaneously applied HHCs in function of time it will be shown in this section what is the additional progress when applying a command on the rotor blade which is not only a function of time but also dependent on the distance along the axis of the blade. The optimization runs performed for this investigations were based on the mathematical model using rigid rotor blades and on the quality criterion defined in section 3.2.2, that is considering also a desired steady state flight path.

### 4.1 Structure for the Time Functions of the distributed Control Inputs

The structure considered here comprises higher harmonic terms up to the 4th HHC in function of the rotation angle $\psi$ (which depends on the time) and in addition a Tschebyscheff- Polynomial in function of the distance r along the axis of the rotor blade:

$$\theta_{add.}(c_{i,j},\psi,r)=[c_{o,o}+\sum_{n=1}^{4} c_{o,2n-1}\cos(n\psi+c_{o,2n})]\cdot T_o(r)$$

$$+[c_{1,o}+\sum_{n=1}^{4} c_{1,2n-1}\cos(n\psi+c_{1,2n})]\cdot T_1(r) \qquad (4.1)$$

$$+[c_{2,o}+\sum_{n=1}^{4} c_{2,n-1}\cos(n\psi+c_{2,2n})]\cdot T_2(r) \quad .$$

In this formula the 27 variables $c_{i,j}$ (i=0,1,2 and j=0,1,2 ...8) are the parameters driven by the optimization algorithm to values minimizing the quality criterion. As visible from this equation the control of the rotor blades is allowed to be time dependent (in function of the angle $\psi$) up to the 4th HHC. The Tschebyscheff-Polynomials $T_o(r)$, $T_1(r)$ and $T_2(r)$ give in addition a distance dependency of the pitch angle along the axis of the rotor blade. These polynomials have the following structure:

$T_o(r)=1$ constant

$T_1(r)=2r-1$ slope

$T_2(r)=2T_1(r)\cdot T_1(r)-T_o$ parabola

. .

. .

. .

$T_n(r)=2T_1(r)\cdot T_{n-1}(r)-T_{n-2}(r)$ polynomial of n th order

with r=coordinate of the distance along the blade axis,
r=o being the root and
r=1 the top of the blade.

For these investigations only a distance dependency up to the 2nd order, that is of parabolic shape, has been chosen.

## 4.2 Results of the Time Dependent and Locally distributed Blade Control

The 27 coefficients of the time dependent and locally distributed control structure (4.1) were driven by the optimization algorithm to the values shown in Table 7.

It is visible that the 3rd time dependent HHC changing the pitch angle along the rotor blade in aparabolic shape (underlined coefficient $\underline{\theta_3}$) exhibits the largest amplitude with the value of $\theta_3=1.138^\circ$. A perspective drawing of these results is shwon in Figure 17, the corresponding topview in Figure 18.

In Table 8 the resulting hub load mean values are shown together with the corresponding fluctuations and deviations from the mean reference values in view to the desired steady state flight path.

The very small fluctuations of the different hub forces and moments are also represented in the Figure 10 and Figure 11 of the preceding paragraph. It is visible that the supplementary locally distributed control of the rotor blades brings a substantial improvement in vibration reduction with a value of $F_{nt}=45.77$ for the sum of the hub reaction fluctuations and a value of $F_{wt}=20.68$ for the quality criterion defined in equation (3.6) which considers also the requirement to hold a desired flight path (see the most right column of Table 8 with the very small deviations of the actual mean values from the desired reference mean values of the hub loads).

## 5. Concluding Remarks

In this paper numerical studies concerning the higher harmonic control of helicopter rotor blades were discussed. Emphasis was placed on the application of the different control methods with single HHC, with several HHC and several HHC with variable twist. The results show that a simultaneous application of the $3\Omega$, $4\Omega$ and $5\Omega$ blade feathering yields the best reduction of the oscillating hub forces and moments. An additional improvment can be obtained with a variable time dependent twist of the rotor blades. The results also show that a single additional $2\Omega$ control causes an umwanted trim state.

Using different mathematical models, it was shown that slightly different results are obtained but the conclusions which can be drawn from this are quite the same.

It is our opinion that further extensions of the mathematical model are necessary e.g. instationary aerodynamics, consideration of more mode shapes, etc to make a significant step foreward to the solution of the true vibratory hub loads but the enormous increase of CPU time is still a major problem.

## 6. List of References


[1] J.L. McCloud, III, An analytical study of a multicyclic controllable twist rotor. Preprint No. 932, 31st Annual National Forum of the American Helicopter Society, Washington, D.C., May (1975).

[2] J.L. McCloud, III and A.L. Weisbirch, Wind-tunnel test results of a full-scale multicyclic controllable twist rotor. Preprint No. 78-60, 34th National Forum of the American Society, Washington, D.C., May (1978).

[3] G. Lehmann, Ermittlung des optimalen periodischen Verlaufs des Einstellwinkels eines Hubschrauber-Rotorblattes. DFVLR, Report No. IB 154-78/12 (1978).

[4] H.G. Jacob, An Engineering Optimization Method with Application to STOL-Aircraft Approach and Landing Trajectories. NASA TN D-6978, Washington , D.C. (1972).

[5] H.G. Jacob, FORTRAN-Programm zur Ermittlung eines lokalen Optimums einer beschränkten multivariablen Gütefunktion ohne Kenntnis ihrer Ableitungen. PDV-Bericht Nr. KFK-PDV 36, Kernforschungszentrum Karlsruhe (1975).

[6] H.G. Jacob, U. Teegen, Zeit- und ortsabhängige suboptimale Steuerung von Systemen mit verteilten Parametern. Regelungstechnik 27 (1979), S. 192-199.

[7] W.von Grünhagen, Bestimmung der gekoppelten Schlagbiege-, Schwenkbiege- und Torsionsschwingungen für beliebige Rotorblätter mit Hilfe der Finite-Element-Methode. DFVLR, Report No. 154-80/21 (1980).

| Control Inputs | Model with Rigid Blades | Model with Elastic Blades |
|---|---|---|
| rotor disk plane angle of attack $\alpha$ | $-8.51^{o}$ | $-8.51^{o}$ |
| $\theta_{o}$ | $8.39^{o}$ | $8.66^{o}$ |
| $\theta_{1c}$ | $1.40^{o}$ | $1.85^{o}$ |
| $\theta_{1s}$ | $-5.63^{o}$ | $-5.09^{o}$ |

Table 1 Control inputs for the steady state flight at $\mu$=0.318 *(computed values for the mathematical models)*

| Hub Loads | Maximum | Minimum | Mean Value | Peak to Peak Distance |
|---|---|---|---|---|
| X(N) | 57.20 | 33.10 | 45.53 | 24.10 |
| Y(N) | -12.66 | -46.40 | -38.59 | 18.45 |
| Z(N) | 3603.48 | 3564.39 | 3583.28 | 39.07 |
| L(Nm) | 11.48 | -15.34 | - 1.54 | 26.83 |
| M(Nm) | 13.21 | -16.21 | - 1.37 | 29.42 |
| N(Nm) | 670.13 | 611.24 | 642.54 | 58.89 |

Table 2 Hub loads in the steady state flight

| Hub Loads | Conventional Control | with 2nd HHC |
|---|---|---|
| X(N) | 45.53 | 73.28 |
| Y(N) | -38.59 | -61.07 |
| Z(N) | 3583.30 | 3665.60 |
| L(Nm) | - 1.54 | -90.90 |
| M(Nm) | - 1.37 | 65.40 |
| N(Nm) | 642.50 | 637.16 |

Table 3 Hub loads in the trim state and with the 2Ω control inputs

| Hub Loads | Mean Value | Peak to Peak Distance | Deviations from Trim |
|---|---|---|---|
| X(N) | 45,14 | 18.14 | -0.39 |
| Y(N) | -38.37 | 22.57 | 0.23 |
| Z(N) | 3583.74 | 16.10 | 0.43 |
| L(Nm) | - 0.97 | 20.94 | 0.57 |
| M(Nm) | - 3.25 | 17.18 | -1.67 |
| N(Nm) | 642,77 | 36.36 | 0,23 |

Table 4 Hub loads with 3rd HHC

| Order n of HHC | $\theta_{o,add}$ | $\theta_{1,add}$ | $\Delta\psi_1$ | $\theta_2$ | $\Delta\psi_2$ | $\theta_3$ | $\Delta\psi_3$ | $\theta_4$ | $\Delta\psi_4$ | $\theta_5$ | $\Delta\psi_5$ | $F_{wt}$ | $F_{nt}$ |
|---|---|---|---|---|---|---|---|---|---|---|---|---|---|
| | conventional control | | | | | | | | | | | 86.6 | 196.8 |
| 1 ÷ 2 | $-0.006^o$ | $-0.017^o$ | $-6.27^o$ | -0.100 | 23.56 | | | | | | | 82.3 | 181.5 |
| 1 ÷ 3 | $-0.006^o$ | -0.011 | $0.78^o$ | -0.060 | -13.25 | -0.284 | $9.78^o$ | | | | | 54.9 | 126.9 |
| 1 ÷ 4 | $-0.003^o$ | 0.009 | $5.12^o$ | -0.060 | -47.40 | -0.23 | $1.55^o$ | -0.084 | -12.93 | | | 44.2 | 103.7 |
| 1 ÷ 5 | $-0.002^o$ | 0.003 | $5.66^o$ | -0.040 | -62.69 | -0.21 | $-6.19^o$ | -0.095 | -15.75 | 0.015 | 3.46 | 41.7 | 99.6 |

Table 5 Amplitudes and phase shifts in dependence of the simultaneously applied HHCs

| Hub Loads | Mean Value | Peak to Peak Distance | Deviation from Trim |
|---|---|---|---|
| X(N) | 46.52 | 13.57 | 0.99 |
| Y(N) | -38.85 | 18.51 | -0.25 |
| Z(N) | 3582.82 | 11.33 | -0.49 |
| L(Nm) | - 3.53 | 21.94 | -1.99 |
| M(Nm) | 1.80 | 18.51 | 3.18 |
| N(Nm) | 641.99 | 19.84 | -0.53 |

Table 6 Hub loads with simultaneous application of four higher harmonics

| | $\theta_{o,add}$ | $\theta_{1,add}$ | $\Delta\psi_1$ | $\theta_2$ | $\Delta\psi_2$ | $\theta_3$ | $\Delta\psi_3$ | $\theta_4$ | $\Delta\psi_4$ | |
|---|---|---|---|---|---|---|---|---|---|---|
| | -0.003 | 0.012 | - 1.20 | 0.093 | -26.51 | -0.049 | - 7.60 | -0.181 | -15.32 | $\cdot T_o(r)$ |
| + | 0.01 | -0.25 | -81.06 | -0.681 | - 0.39 | -0.004 | - 8.04 | -0.206 | 62.70 | $\cdot T_1(r)$ |
| + | -0.023 | 0.083 | 3.02 | 0.146 | 38.59 | 1.138 | -89.65 | -0.028 | 2.07 | $\cdot T_2(r)$ |

Table 7 Optimal coefficients of the time dependent and locally distributed control structure

| Hub Loads | Mean Value | Peak to Peak Distance | Deviation from Trim |
|---|---|---|---|
| X(N) | 44.67 | 12.36 | -0.86 |
| Y(N) | -38.57 | 12.11 | 0.02 |
| Z(N) | 3582.93 | 3.47 | -0.37 |
| L(Nm) | - 1.58 | 6.63 | -0.04 |
| M(Nm) | - 1.02 | 4.60 | 0.36 |
| N(Nm) | 643.25 | 6.58 | 0.72 |

Table 8 Hub loads with time dependent and locally distributed blade control

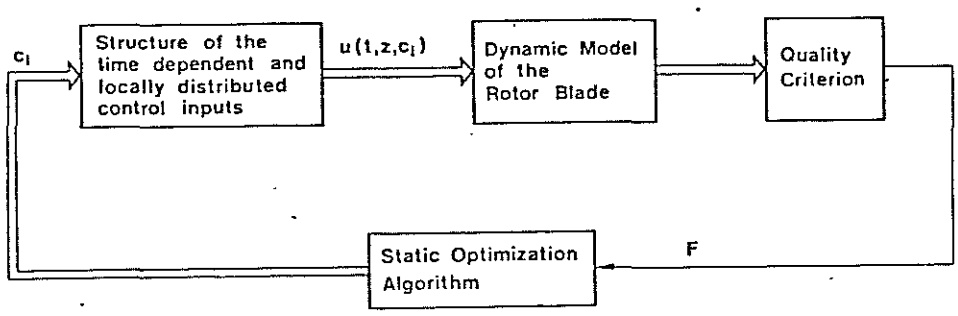


Fig. 1 Principle of the Optimization procedure

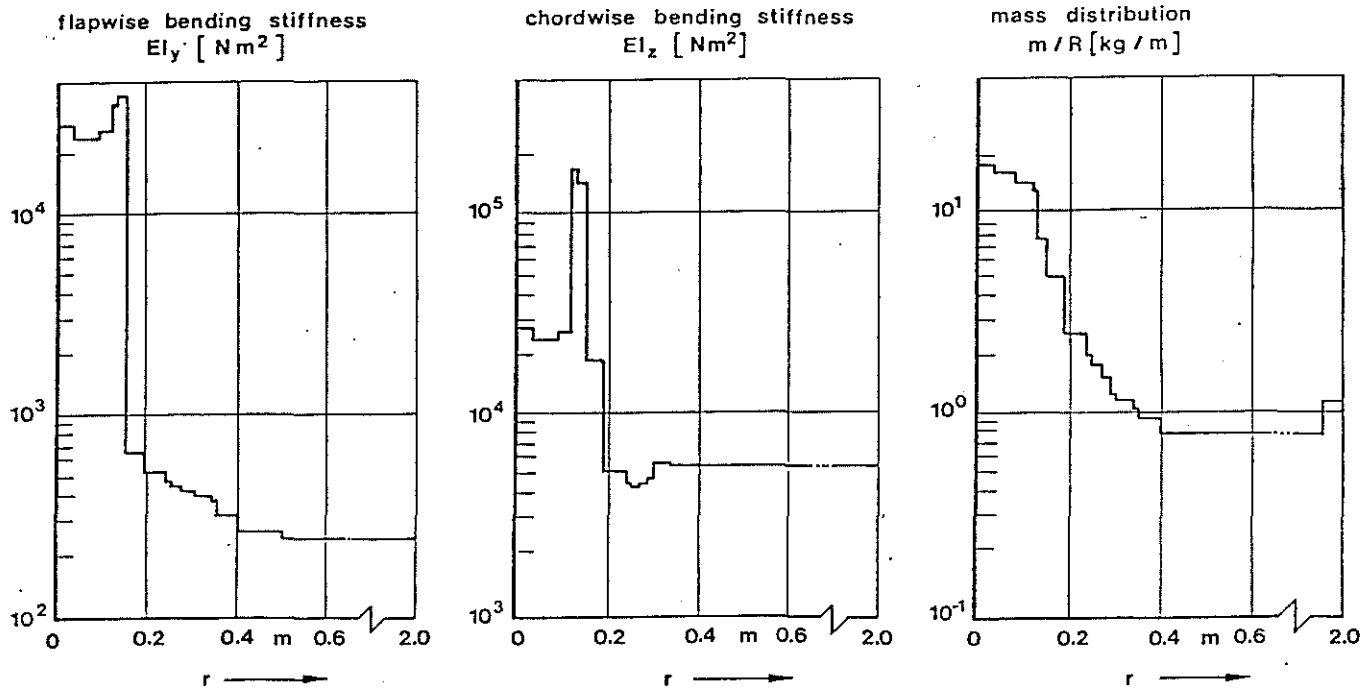


Fig. 2 Stiffness and mass distributions of the model rotor blade

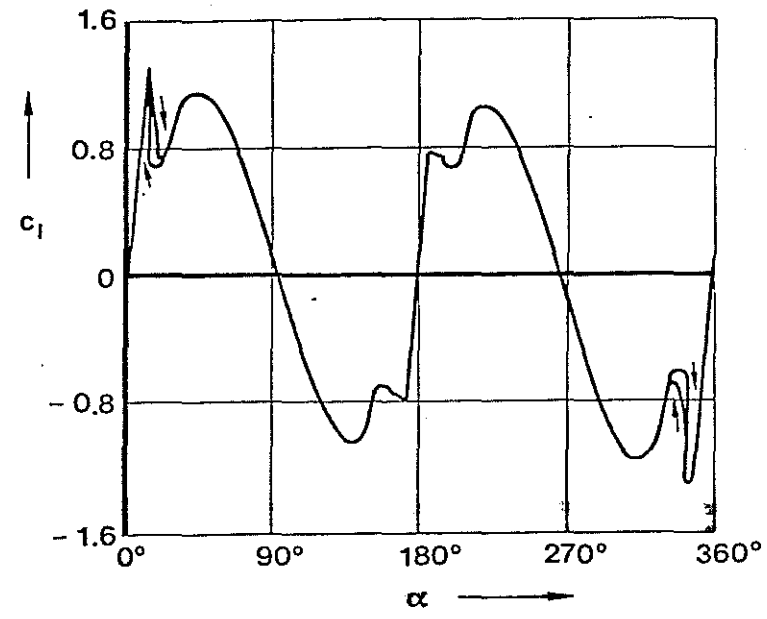


Fig. 3 Lift coefficient versus angle α for the NACA 0012 airfoil [NACA TN 3361]

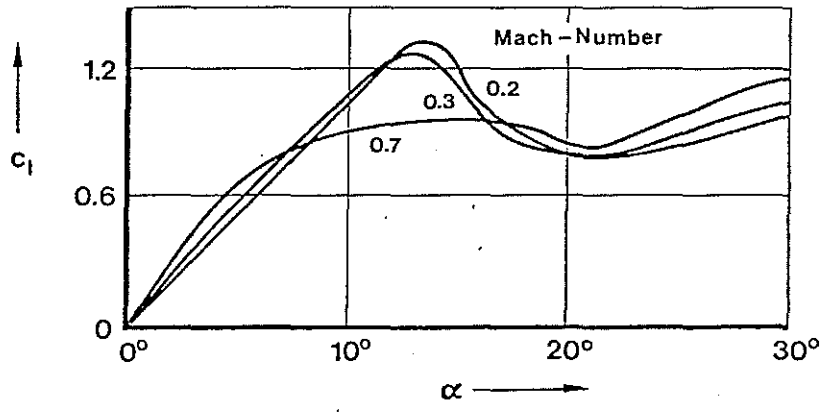


Fig. 4 Lift coefficient versus angle α for the NACA 0012 airfoil [NACA TN 3361]

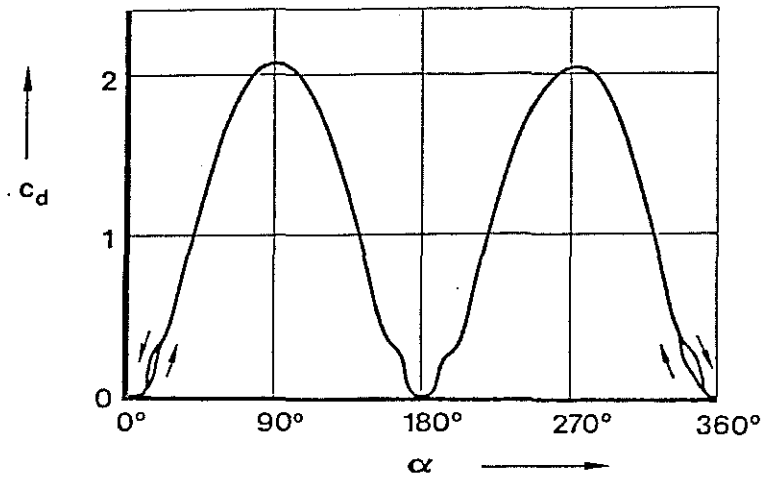


Fig. 5 Drag coefficient versus angle α for the NACA 0012 airfoil [NACA TN 3361]

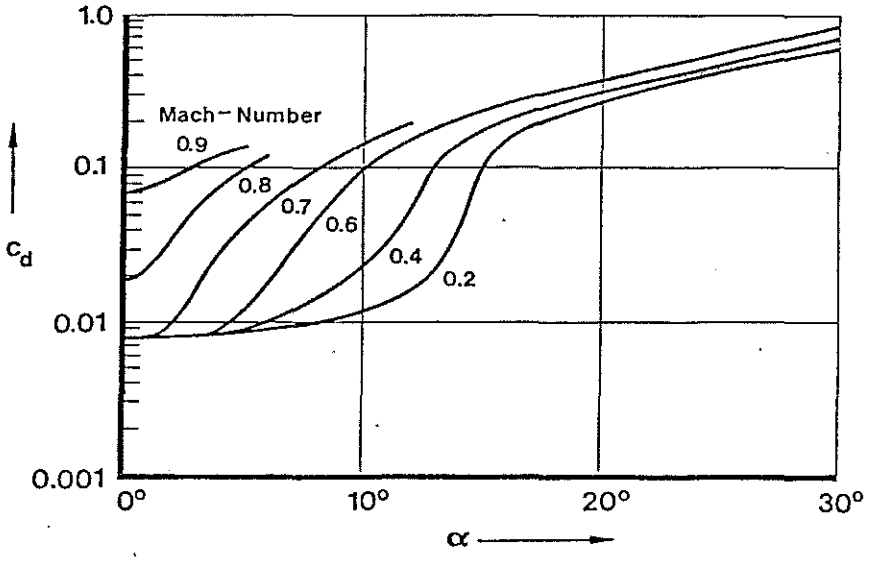


Fig. 6 Drag coefficient versus angle α for the NACA 0012 airfoil [NACA TN 3361]

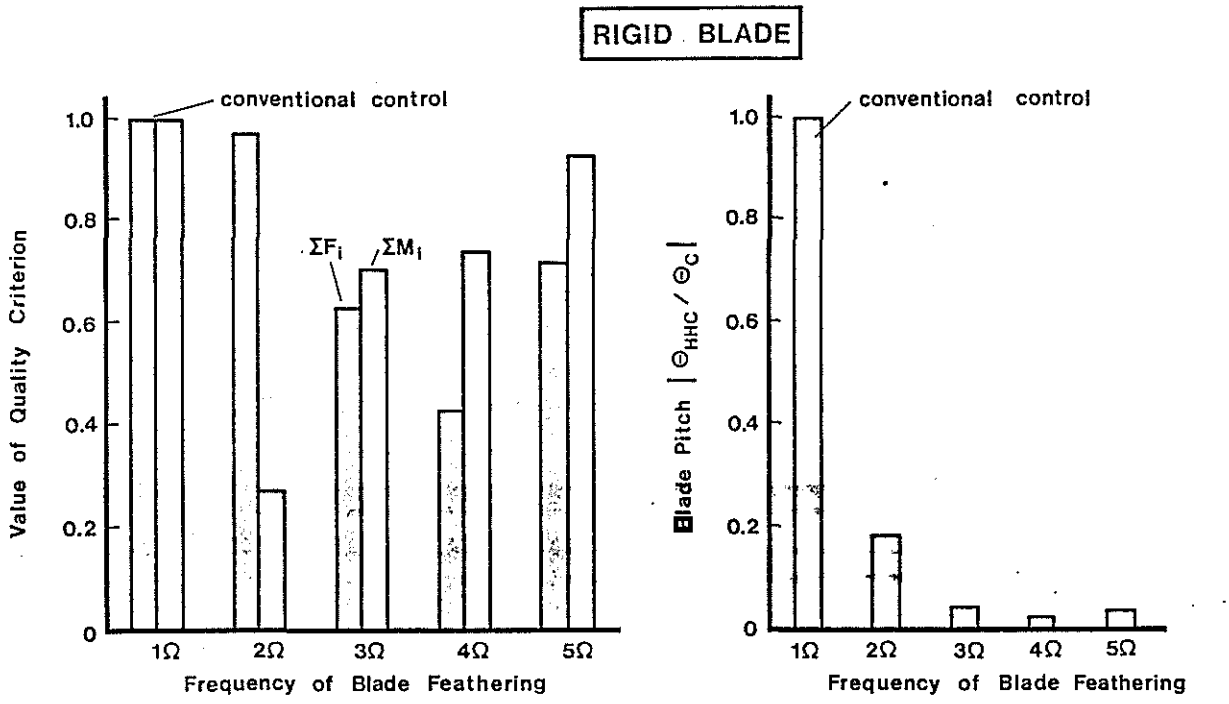


Fig. 7 Values of the optimized quality criterion and the corresponding input amplitudes for the rigid blade model and single higher harmonic control inputs

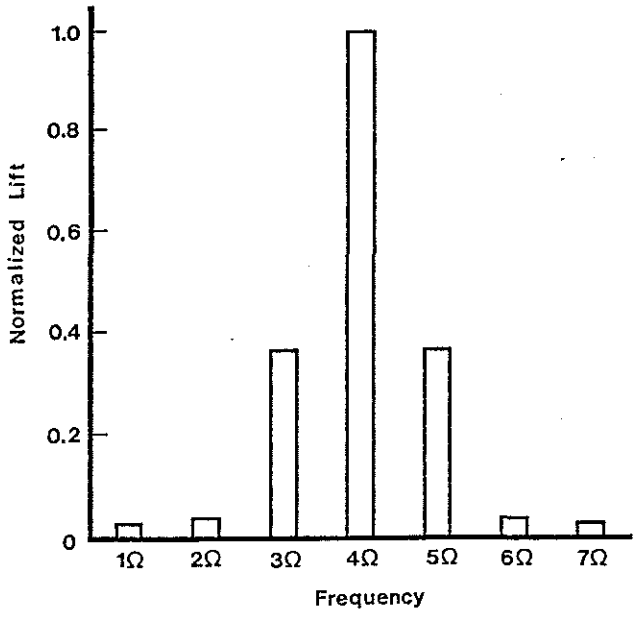


Fig. 8 Spectrum of aerodynamic loads caused by 4Ω blade feathering

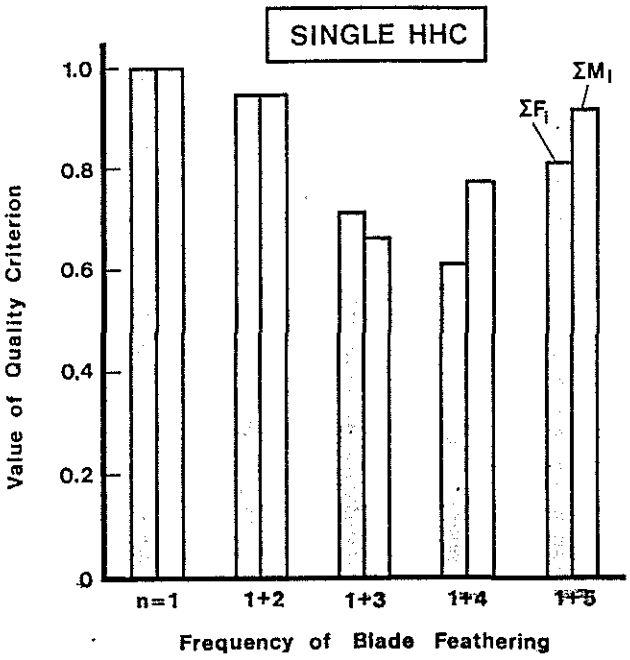


Fig. 9 Reduction of the hub reaction fluctuations with single higher harmonic control

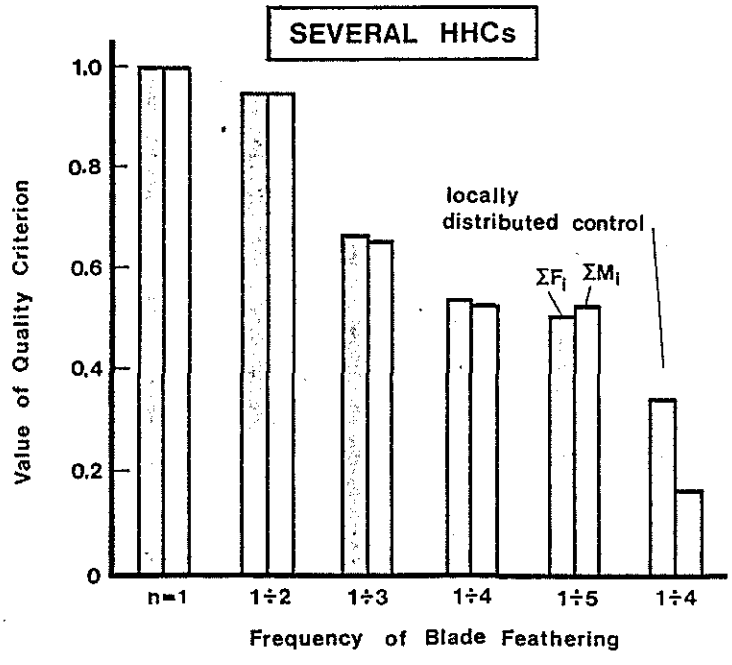


Fig. 10 Reduction of the hub reaction fluctuations with several HHCs applied simultaneously

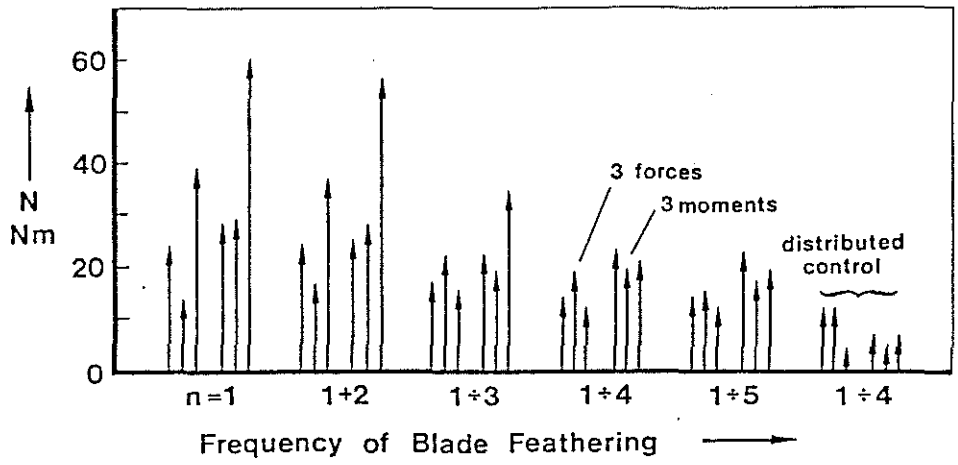


Fig. 11 Reduction of hub load fluctuations with simultaneous higher harmonic control

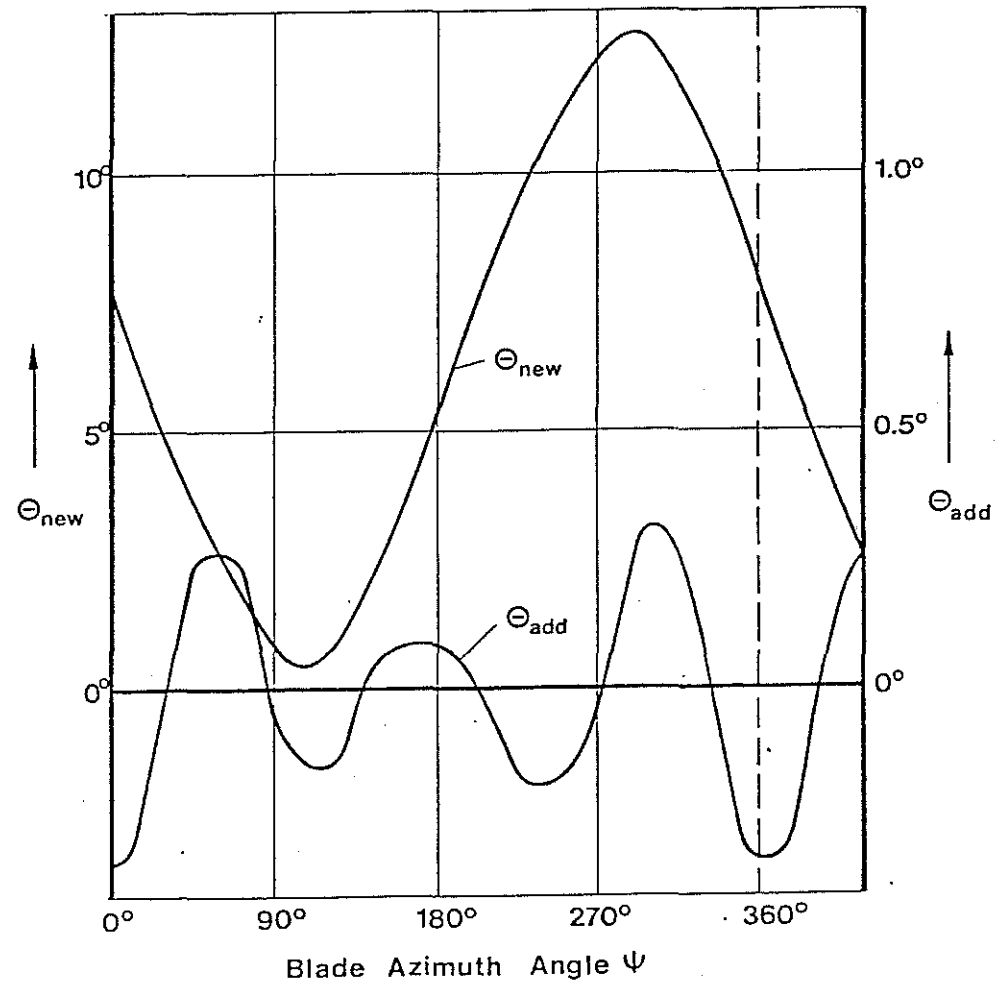


Fig. 12 Evolutions of $\theta_{add}(\psi)$ and of $\theta_{new}(\psi)$ for an input up to the 4th HHC

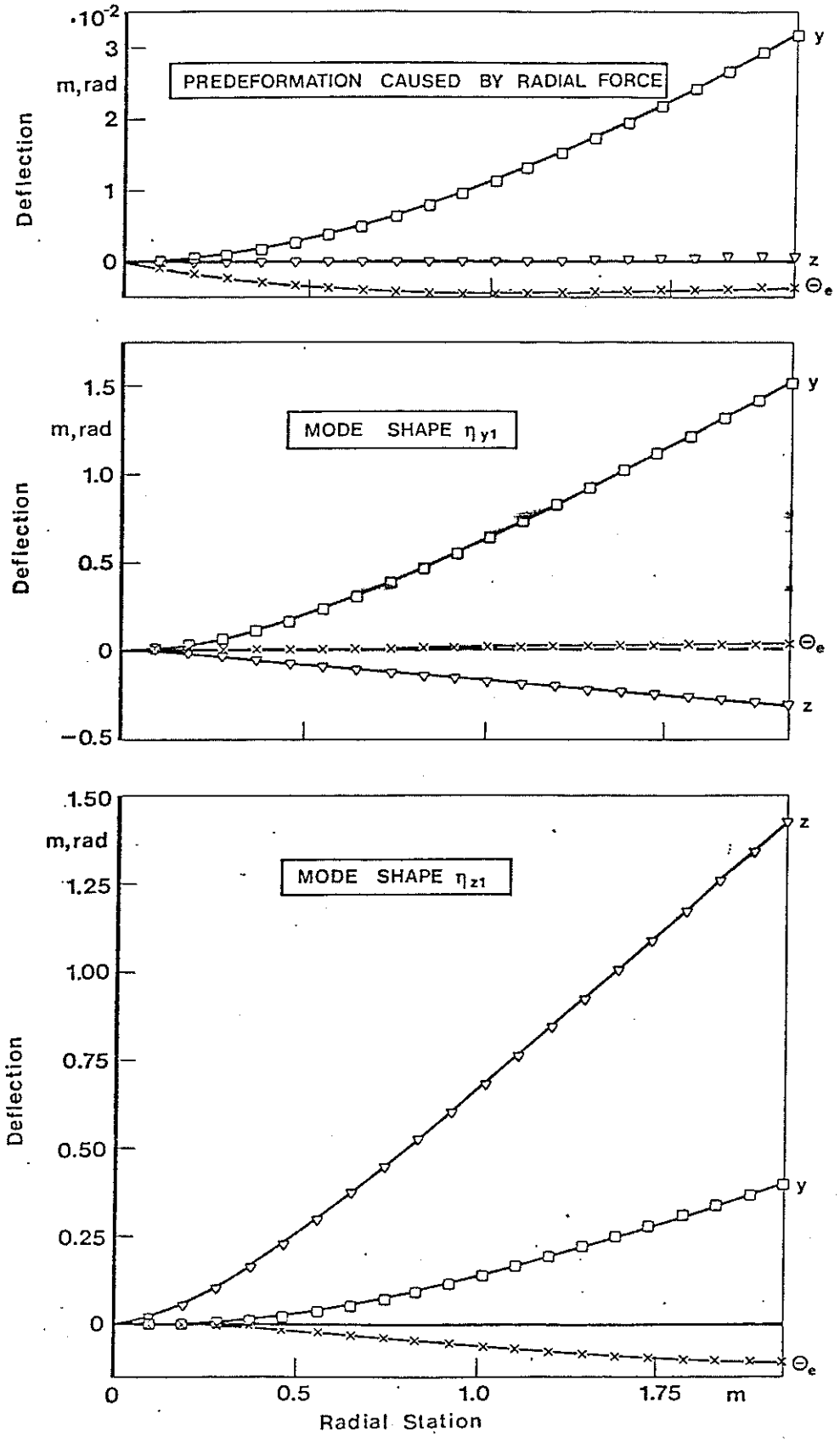


Fig. 13 First mode shapes of the model rotor blade

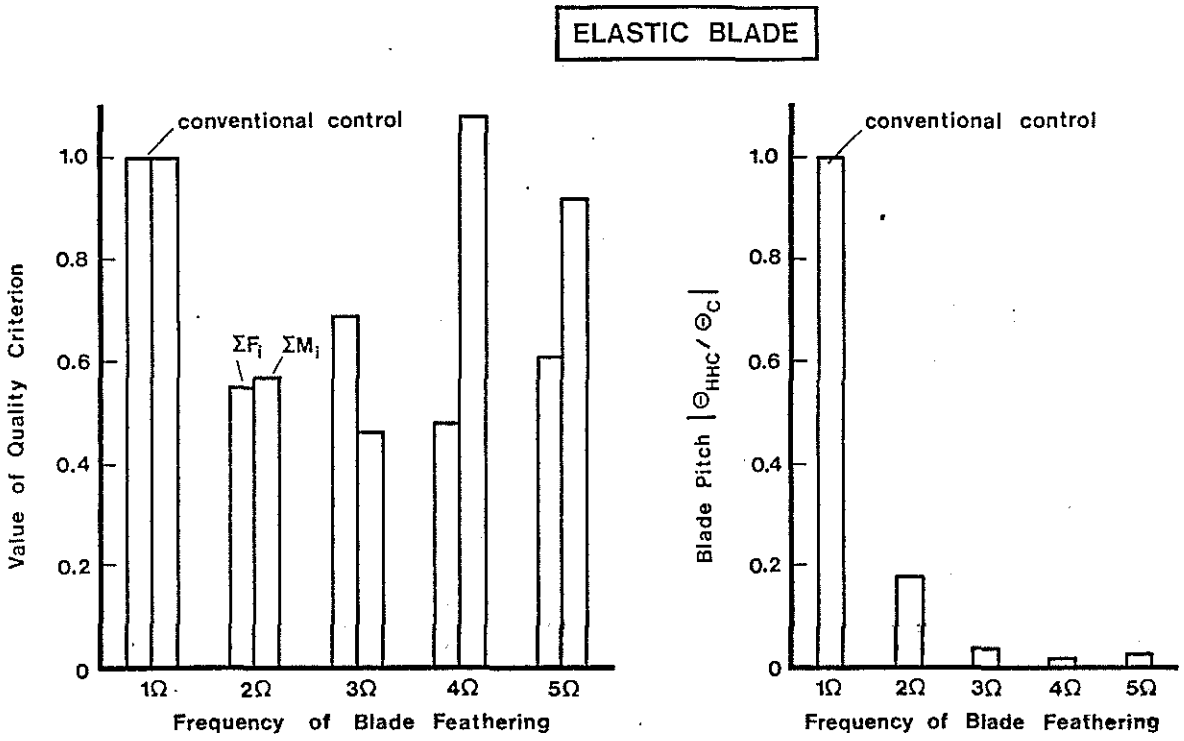


Fig. 14 Values of the optimized quality criterion and the corresponding input amplitudes for the elastic blade model and single higher harmonic

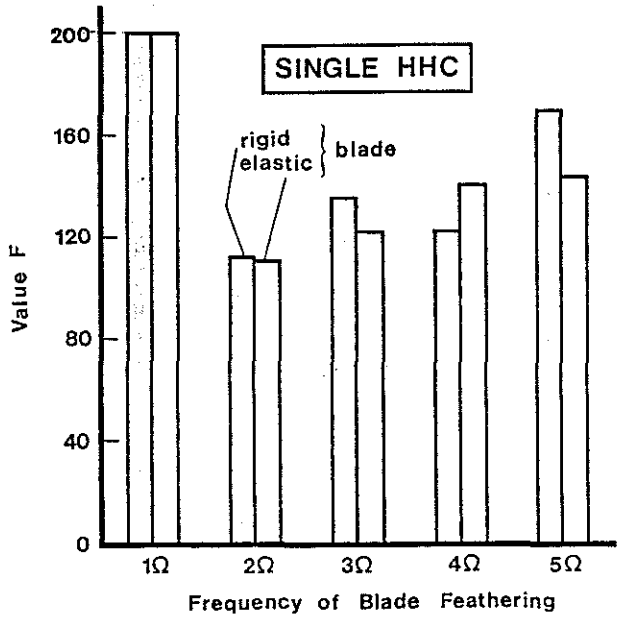


Fig. 15 Reduction of the oscillating hub loads yielded by single HHC

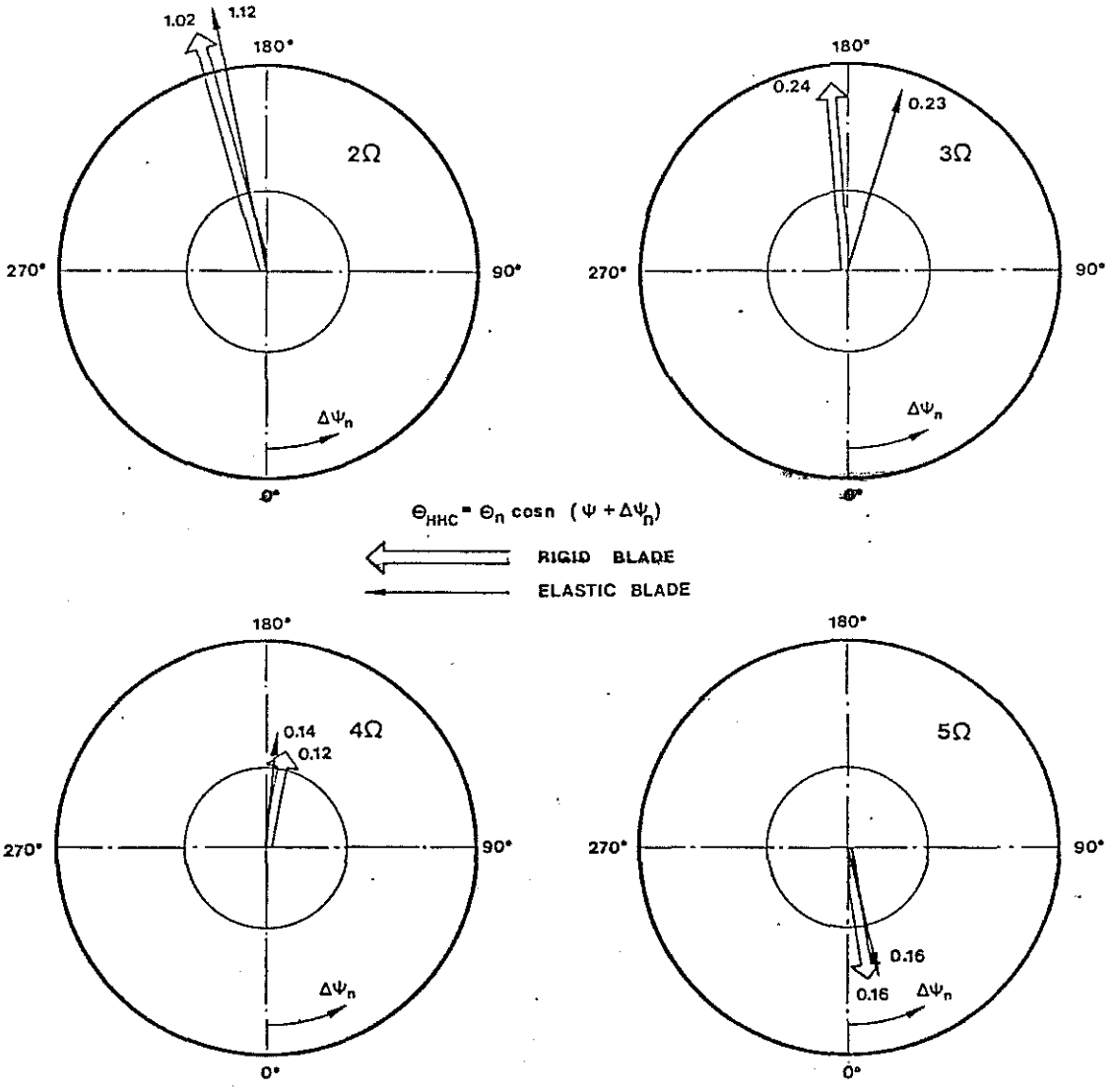


Fig. 16 Optimal control inputs for single HHC

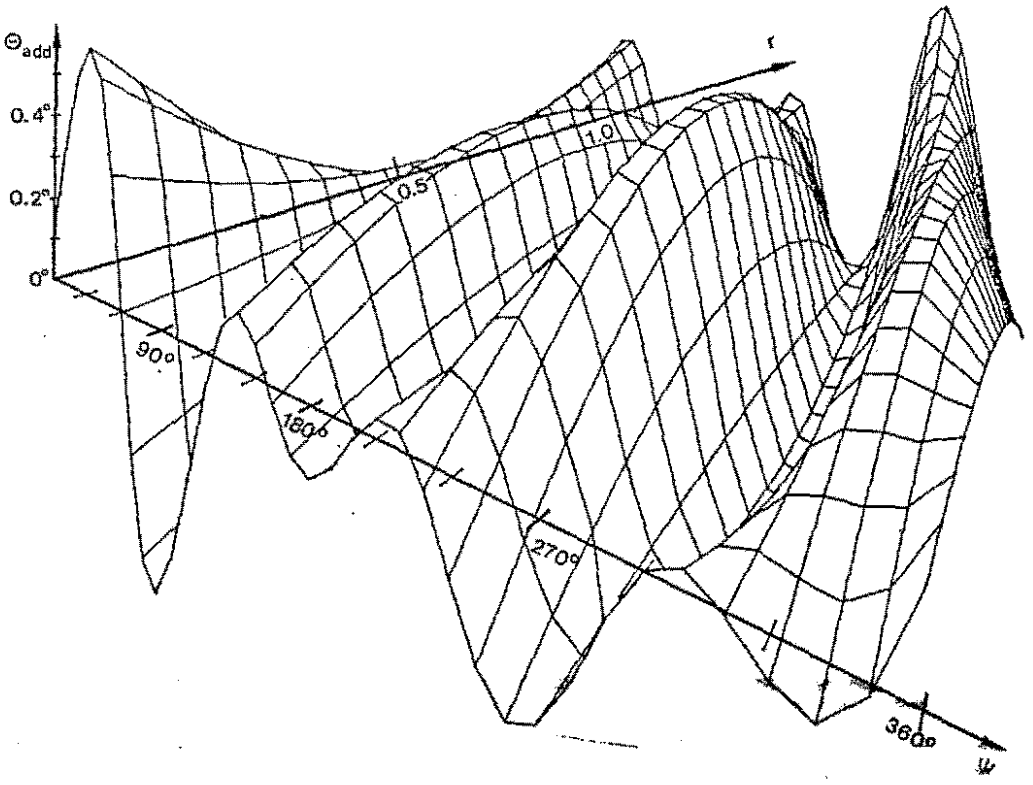


Fig. 17 Additional optimal control inputs versus the azimuth angle $\psi$ and the radial station r

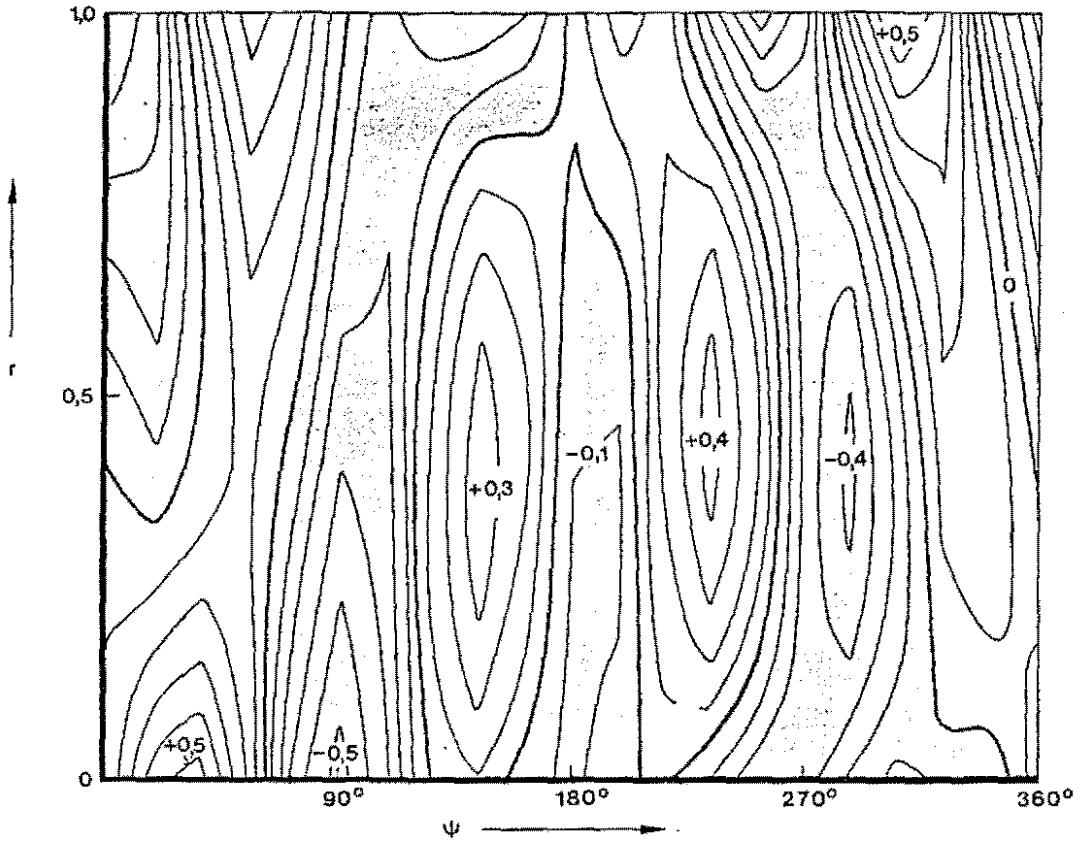


Fig. 18 Topview of Fig. 17